Short-wavelength soft-x-ray amplification in a lithiumlike calcium plasma

Z. Z. Xu, P. Z. Fan, L. H. Lin, Y. L. Li, X. F. Wang, R. X. Li,
P. X. Lu, S. S. Han, L. Sun, A. D. Qian, Z. Q. Zhang, and J. Z. Zhou
Shanghai Institute of Optics and Fine Mechanics, Academia Sinica, P.O. Box 800-211, Shanghai 201800, People's Republic of China
(Received 1 February 1993)

In this paper, we present the results of an x-ray-laser gain experiment on Li-like Ca^{17+} ions, conducted recently at the LF12 Laser Facility of the Shanghai Institute of Optics and Fine Mechanics with a CaF_2 slab target, and the time histories of amplified spontaneous emission in Li-like x-ray lasers at different distances from the target surface.

PACS number(s): 42.55.Vc, 32.70.−n, 52.50.Jm

I. INTRODUCTION

The lithiumlike ion scheme of the recombination pumping x-ray laser has manifested its great advantages in extending x-ray lasers to short-wavelength range, namely, the water window (43.8–23.3 Å). For a given lasing wavelength, its required driving laser power is not only much lower than that for the electron collisional pumping mechanism, but also lower than that for the hydrogenlike ion scheme of the recombination pumping mechanism. The values $V_i/h\nu$, i.e., the ratios of the ionization potential to the lasing transition energy for the H-like, the Li-like, and the Na-like schemes of the recombination mechanism are given in Table I, together with that for the neonlike and the nickellike schemes of the electron collisional mechanism for comparison. We can see from the table that for the same lasing wavelength, besides the Na-like scheme, the Li-like scheme has the smallest value $V_i/h\nu$ among these main pumping schemes. As a consequence, the Li-like scheme requires a lower plasma temperature and hence a lower pumping power. Furthermore, it can be scaled to short wavelength with nuclear charge Z more rapidly ($\lambda \sim Z^{-2.5}$) than the H-like scheme ($\lambda \sim Z^{-2}$). Therefore, by using the Li-like scheme, the x-ray lasers with wavelength near or in the water window may be expected by using a medium-scale, or even a small-scale, laser facility as a driver, i.e., the compact, moderate cost and so-called "table-top" x-ray lasers may be made available.

TABLE I. $V_i/h\nu$ for main pumping schemes of x-ray lasers.

Pumping mechanism	Pumping scheme	Lasing transition	$V_i/h\nu$
Collisional	Ne-like	3*p*-3*s*	~45
	Ni-like	4*d*-4*p*	~15
Recombination	H-like	3-2	7.2
	Li-like	4*f*-3*d*	6.4–5.4
	Li-like	5*f*-3*d*	4.4–3.7
	Na-like	6*g*-4*f*	~3.9

The recombination pumping soft x-ray lasers of the Li-like ions have been initially investigated experimentally by Jaegle *et al.* [1]. Recently, a number of laboratories in the world have also carried out the investigation on the Li-like recombination x-ray lasers [2–7]. At the Shanghai Institute of Optics and Fine Mechanics (SIOFM) Xu and co-workers have also successfully carried out the recombination soft-x-ray-laser gain experiments [8–10] of the Li-like aluminum and silicon ions and obtained experimental evidence of the amplification of spontaneous emission (ASE) for Al^{10+} 5*f*-3*d* (105.7 Å), 4*f*-3*d* (154.6 Å) and Si^{11+} 5*f*-3*d* (88.84 Å), 5*d*-3*p* (87.28 Å), 6*f*-3*d* (75.83 Å), and 6*d*-3*p* (74.64 Å) transitions at much lower driving laser intensity. We have observed the gain reduction for longer and wider plasma columns and obtained the spatial distribution of the gain along the normal of the target surface and dependence of the gain on the driving laser intensity on the target surface. We also observed the soft-x-ray amplification for the 6*g*-4*f* (72.22 Å) of the Na-like Cu^{18+} ions for the first time [11].

In this paper we will present the experimental results on the short-wavelength Li-like x-ray laser research of Xu and co-workers. In our present experiment, the soft-x-ray laser was extended to the higher-Z elements by using CaF_2 slab targets, and the soft-x-ray amplification of the Li-like Ca^{17+} 4*f*-3*d* transition was successfully demonstrated, the wavelengths being 57.7 Å. We also observed the amplification of the F^{8+} 3-2 (80.9 Å) transition of the H-like fluorine ions. The spatial and temporal behaviors of ASE emission in the Li-like lasers were also obtained by using a soft-x-ray streak camera.

II. EXPERIMENTAL ARRANGEMENT

The short-wavelength Li-like soft-x-ray-laser experiment was carried out at the LF12 Laser Facility of SIOFM. In the experiment, only the north beam of this two-beam facility was used to produce line-shaped plasmas as lasing medium. The energy of the 1.05 μm laser beam was about 550 J and the duration (FWHM) of the quasi-Gaussian pulse was about 900 ps.

The experimental arrangement was essentially the same as the one used previously [10]. Figure 1 shows the schematic of the experimental setup. Briefly, the line

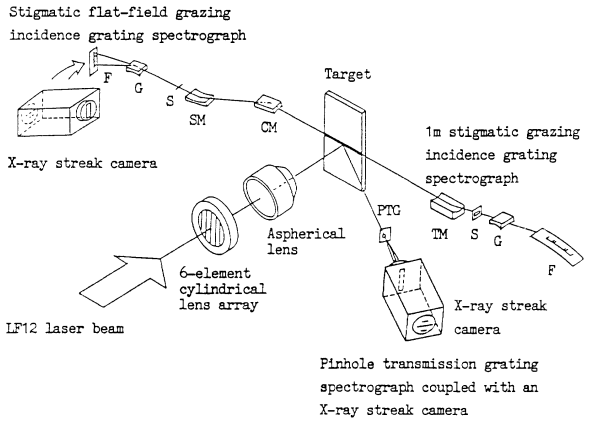

FIG. 1. Experimental arrangement. TM: toroidal mirror; CM: cylindrical mirror; SM: spherical mirror; S: slit; G: grating; F: film.

focus system, an $f/1.7$ aspherical lens combined with a cylindrical lens array formed a line focus of 12.5 mm in length and 120 μm in width on the slab targets. The laser intensity on the target surface was about 4.0×10^{13} W/cm^2. The targets used in the experiment were all 5-mm-thick CaF_2 slabs with polished surfaces. The lengths of the targets were 2, 4, 6, 8, and 10 mm. The primary diagnostic equipment used in the experiment was a stigmatic grazing-incidence flat-field grating spectrograph [12,13], which was composed of a grazing-incidence flat-field grating spectrograph and a grazing-incidence collecting optics consisting of a cylindrical mirror and a spherical mirror. The key component of the spectrograph was a variable line-spacing concave grating: $r=5649$ mm, gold coated, 3.2° blaze angle and 1/1200 mm nominal groove spacing, supplied by Hitachi Company. When the incidence angle is 87° and the slit is set 237 mm from the grating apex, the spectrum can be formed sharply on the focal plane at 235 mm from the apex of the grating and cover the wavelength from 44 to 300 Å over a focal plane about 40 mm in length, with a 0.1 Å spectral resolution. The grazing-incidence collecting optics can not only provide high efficiency but also compensate the astigmatism and thus form a stigmatic spectrum. Because the imaging distance varies only slightly with the wavelength, a one-dimensional spatially resolved spectrum can be obtained with good quality in the whole wavelength range from 44 to 300 Å. The radii of the cylindrical and the spherical mirrors were 20 and 3000 mm, respectively, and the mirrors were gold coated. In the experiment, the optical axis of the spectrograph was aligned with the axis of the line-shaped plasma, the slit of the spectrograph was parallel to the normal of the target (i.e., the axis of the driving laser beam) and thus the obtained spectrum has one-dimensional spatial resolution along the normal of the target surface. The spatial amplification of the system was about 2. At constant laser irradiance on the targets, the axial intensities for different plasma columns were measured and thus was obtained the gain coefficient for the lasing lines. In the gain experiment, we used soft-x-ray film (5 FW) provided by Shanghai Film Factory as the detector for attaining time integrated and spatially resolved spectra. The film has been calibrated recently.

In a time-resolution experiment, we used the photocathode of the soft-x-ray streak camera [14] provided by Xian Institute of Optics and Fine Mechanics as the detector. In the experiment, the soft-x-ray streak camera was so adjusted that the scanning slit (18 mm in length and 200 μm in width) in front of the photocathode was set parallel with the dispersion axis of the spectrum and to cover the desired part of the spectrum. The 18-mm-long scanning slit of the streak camera can cover $\sim$50 Å wavelength range. Because the spatial amplification of the system was 2, the 200 μm width of the scanning slit corresponded to 100 μm region in the source. By changing the position of the target surface and keeping the relative position of the streak camera to the flat-field grating spectrograph unchanged, the time-resolved spectrum at different distances from the target surface can be obtained. The photocathode of the soft-x-ray streak camera was low density CsI which can respond to the XUV radiation of interest.

At the other end of the plasma column, namely, the opposite side of the grazing-incidence flat-field grating spectrograph, was positioned a Rowland-circle grazing-incidence grating spectrograph for obtaining the axial spectra or the *in situ* calibration of the film. A pinhole-transmission-grating spectrograph was positioned 35° with the normal of the target (in the same horizontal plane as the axis of the driving laser), the diameter and line spacing of the pinhole-transmission grating being 25 μm and 1/2000 mm, respectively, for monitoring the uniformity of the plasma along its axis (using the film recording) and the time history of the emission from the plasma (using the soft-x-ray streak camera recording), and sometimes for film calibration. Two flat-crystal x-ray spectrographs, one with a pinhole, were also used to monitor the x-ray emission of the plasma column. In addition, an optical imaging diagnostic system was used to obtain the micrographs of the $\omega_0, 2\omega_0, 3\omega_0/2$ emission profiles of the plasma, simultaneously, so as to examine the uniformity of the plasma column.

III. EXPERIMENTAL RESULTS AND DISCUSSION

One-dimensional spatially resolved spectra for CaF_2 slab targets were obtained with the stigmatic grazing-incidence flat-field grating spectrograph with a slit of 10 μm on 5 FW film. Figure 2 is the microdensitometer trace for a 10-mm plasma column. Spectral identification showed that the axial spectra of the line-focused laser plasma of the CaF_2 target was dominated by the spectral lines originating from the transitions of the Li-like Ca^{17+} ions and the H-like F^{8+} ions. There are also spectral lines originating from other ions, but these spectral lines are much weaker. The experimentally measured wavelengths for Ca^{17+} ions were in good agreement with the calculated wavelengths [10].

The relative line intensities were determined from the photographic densities with the relative calibration curve of 5 FW film by the normal procedure of the spectral in-

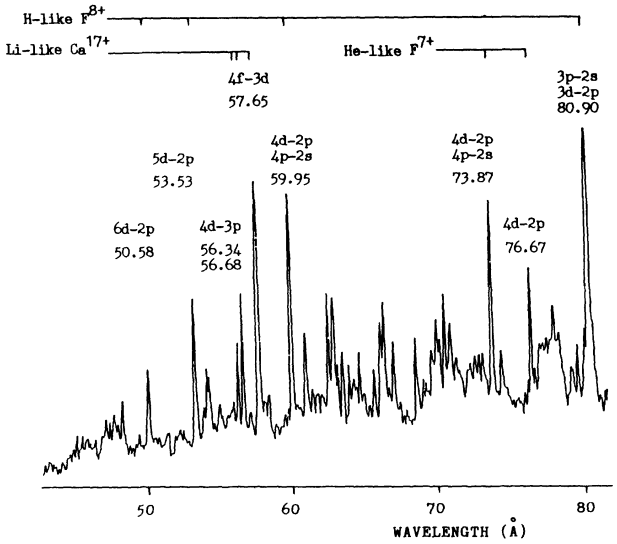

FIG. 2. Microdensitometer trace of CaF_2 axial spectrum (10 mm). The transition wavelengths (in Å) are given for several peaks.

tensity measurement. The relative intensities for Ca^{17+} $4f$-$3d$ (57.7 Å) at four different distances from the target surface as a function of the plasma length L are shown in Fig. 3. These figures show that the intensities for the Ca^{17+} $4f$-$3d$ transition increase nonlinearly with plasma length. A least-square fit to the Linford equation: $I=I_0(e^{GL}-1)^{3/2}/(GLe^{GL})^{1/2}$ yielded gain coefficients G of 4.3, 3.8, 2.6, and 0.9 cm^{-1} at distances of 150, 170, 210, and 350 μm from the target surface, respectively. In the same way, we obtained the maximum gain coefficient of 1.4 cm^{-1} at 220 μm from the target for the F^{8+} 3-2 transition.

Our previous experiment [10] indicated that there exists a gain distribution along the normal of the target: starting from the target surface, a negative gain (i.e., absorption) appears first; at some distance, the absorption turns to the amplification and gain emerges, then the gain reaches its peak value and then gradually decreases with the increasing distance from the target. The distance at which the gain reaches its maximum value is 150 μm for Ca^{17+} $4f$-$3d$. In comparison with previous results for Si^{11+}, the region having maximum gain is moved towards the target, indicating that the place having the maximum gain depends on the nuclear charge Z of the lasing ions.

Using the isoelectronic scaling of the recombination Hα lasers for reference, where the driving laser intensity is scaled as $I\sim Z^4$ [15], there is a similar isoelectronic scaling for the recombination Li-like ion lasers as $I\sim(Z-2)^4$. In the soft-x-ray-laser experiment of the Li-like Si^{11+} ions, we have investigated the dependence of gain on the laser intensity in detail and found the optimal laser intensity on the target for Si^{11+} $5f$-$3d$ (88.84 Å) was 2.5×10^{12} W/cm^2. Based on the isoelectronic scaling for the Li-like scheme, the optical laser intensity for Ca^{17+} should be 1.3×10^{13} W/cm^2. In the preliminary experiment, considering the laser energy losses in focusing optics, the intensity $\sim4\times10^{13}$ W/cm^2 was chosen for the CaF_2 target. Obviously, a systematic experiment should be carried out for determining the optimal laser intensity. It should be noticed that the pulse duration of the driving laser and the width of the line focus used in the experi-

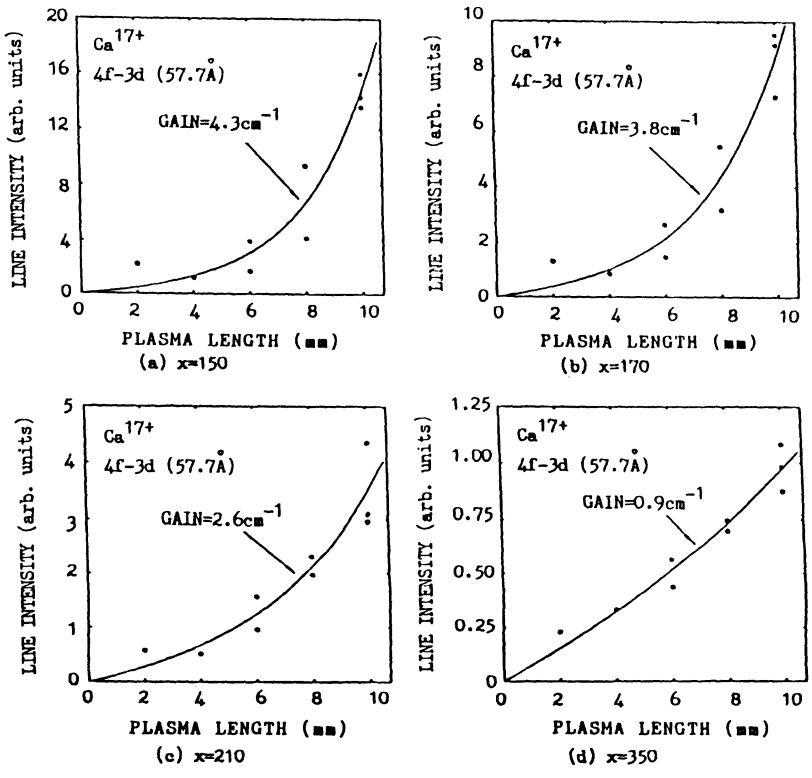

FIG. 3. Relative intensity vs plasma length for Ca^{17+} $4f$-$3d$ at four distances X (μm) from target surface.

ment are apparently far from being desirable. The pulse duration of the driving laser and the width of the line focus should be much narrower as the atomic number increases and the lasing wavelength decreases. These are the important issues to be solved in the future work on the Li-like recombination lasers. We have done something to reduce the width of line focus and pulse duration of the driving laser.

Although we have observed the spectral line of Ca^{17+} $5f$-$3d$ (~39 Å) transition, the line was broad and weak, due to serious defocusing for the lines below 44 Å in our spectrograph. In a future experiment we will use 2400 grooves per variably spaced grating to obtain a good spectrum below 44 Å. We expect that it is possible to use the Ca^{17+} $5f$-$3d$ transition to achieve the recombination soft-x-ray laser in the water window.

As mentioned above, by coupling the stigmatic grazing-incidence flat-field grating spectrograph with the soft-x-ray streak camera, we can obtain the time-resolved spectra emitted in an ~100-μm region at different distances from the target. We assumed that the onset of the zeroth order of the transmission grating streak spectrum coincides with the beginning of the driving laser pulse. Changing the delay but keeping the other operating conditions of the streak camera the same, we measured the time-resolved spectra from both the transmission grating and the flat-field grating spectrographs. Comparing the two time-resolved spectra, we could determine the timing of x-ray lasing relative to the driving laser pulse. The time-resolved spectra displayed on the screen of the image amplifier of the streak camera were recorded on Lucky film (ASA400-27DIN), which was supplied by No. 1 Film Factory of the Ministry of Chemistry Industry in Baoding, China, and which has been calibrated separately. The spectral resolution in the time-resolved spectrum was reduced to ~0.5 Å at 80 Å due to the limited spatial resolution of the image amplifier. A typical streaked spectrogram is shown in Fig. 4. By converting the film density into relative intensity and subtracting the continuum background nearby, we can obtain the time history for each spectral line. The time histories for the Li-like Si^{11+} $5f$-$3d$ (88.84 Å), $5d$-$3p$ (87.28 Å), $6f$-$3d$ (75.83 Å), and $6d$-$3p$ (74.64 Å) lasing at distances 200 and 400 μm from the target are given in Fig. 5. From the figure we can see that the x-ray lasing of the Li-like ions always appears after the driving laser pulse and has long duration. These manifest the time and space characteristics of the recombination pumping x-ray lasing: after heating and producing highly ionized plasma by the interaction of the driving laser beam with the target, the plasma is cooling rapidly by adiabatic expanding and radiation. This enhances the three-body recombination and leads to population inversion and lasing. The lasing duration and delay relative to the driving laser pulse were of the order of nanoseconds in our case. The experimental results also showed that the delay and duration for the distance 400 μm from the target were longer than that for the distance 200 μm from the target. In the experiment, we also investigated preliminarily the time and space characteristics of the lasing lines of the Li-like Ca^{17+} ions and the H-like F^{8+} ions. The time histories for two lasing lines, Ca^{17+} $4f$-$3d$ (57.7 Å) and F^{8+} 3-2 (80.9 Å) of the CaF_2 target are shown in Fig. 6. The results show that the delay of the Ca^{17+} $4f$-$3d$ lasing relative to the driving laser pulse was apparently shorter, while the delay of the F^{8+} 3-2 lasing was about the same as the one for the Li-like Si^{11+} lasing. The time delay and long duration of the Li-like lasing, different apparently from the time behaviors of x-ray lasing pumped by the electron collisional mechanism, demonstrated that the emission of the recombination laser always appears after the driving laser pulse and has long durations which are favorable for achieving mul-

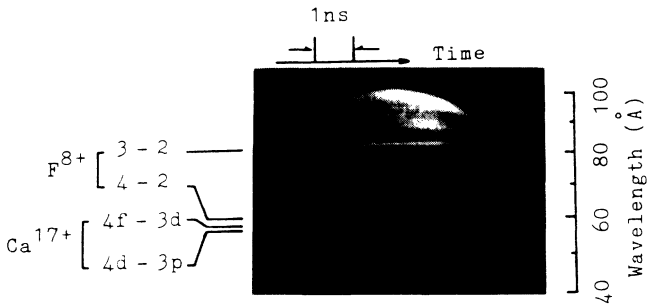

FIG. 4. Axial streaked spectrogram at distance 250 μm from target surface for 10-mm CaF_2 slab target.

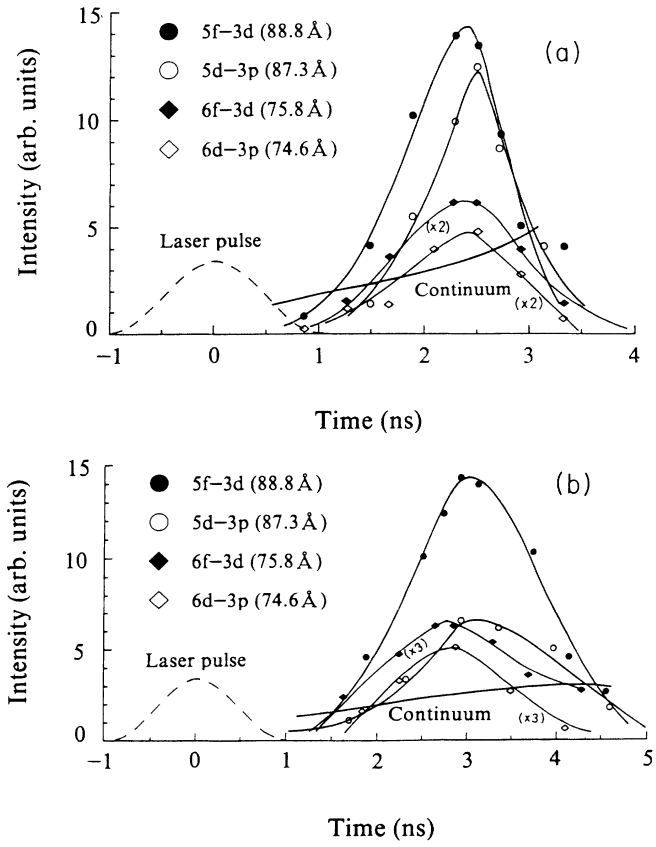

FIG. 5. Time histories of Si^{11+} x-ray lasing lines for spatial region (a) 150–250 μm, (b) 350–450 μm from target surface at 2.5×10^{12} W/cm^2 intensity.

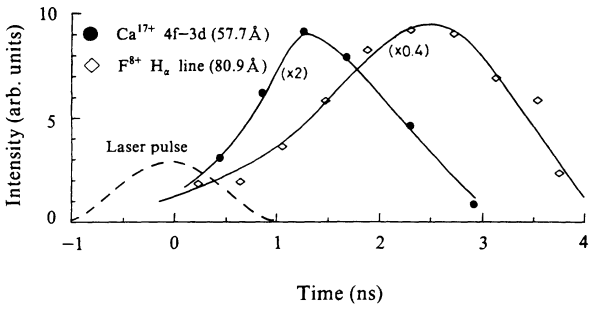

FIG. 6. Time histories for Ca^{17+} 4*f*-3*d* and F^{8+} 3-2 lasing lines for spatial region 200–300 μm from target surface at 2×10^{13} W/cm^2 intensity.

tipass amplification and improving the laser performance by using an x-ray mirror.

IV. SUMMARY

In the experiment on the recombination soft-x-ray laser with CaF_2 slab targets, soft-x-ray amplification of the Ca^{17+} 4*f*-3*d* (57.7 Å) and the F^{8+} 3-2 (80.9 Å) transitions has been observed, the measured maximum gain coefficients being 4.3 and 1.4 cm^{-1}, respectively. Preliminary observations of the spatial and temporal behaviors of the Li-like lasing were made by using the stigmatic grazing-incidence flat-field grating spectrograph coupled with the soft-x-ray streak camera. The results of the experiments showed that the Li-like ion scheme has great potential in achieving the recombination soft-x-ray lasers in the water window.

ACKNOWLEDGMENTS

The authors gratefully acknowledge the LF12 Laser Facility Operation Group for their assistance and cooperation and the Shanghai Film Factory for their providing Shanghai 5F x-ray film without a supercoat. This work was supported by the National Nature Science Foundation and the National High Technology Program of China.

[1] P. Jaegle, G. Jamelot, A. Carillon, A. Klisnick, A. Sureau, and H. Guennou, J. Opt. Soc. Am. B **4**, 563 (1987).
[2] C. L. S. Lewis, R. Corbett, D. O'Neil, C. Regan, S. Saadat, C. Chenais-Popovics, T. Tomie, J. Edwards, G. P. Kiehn, R. Smith, O. Willi, A. Carillon, H. Guennou, P. Jeagle, G. Jamelot, A. Klisnick A. Sureau, M. Grande, C. Hooker, M. H. Key, S. J. Rose, I. N. Ross, P. T. Rumsby, G. J. Pert, and S. A. Ramsden, Plasma Phys. Controlled Fusion **30**, 35 (1988).
[3] P. R. Herman, T. Tachi, K. Shihoyama, H. Shiraga, and Y. Kato, IEEE Trans. Plasma Sci. **16**, 520 (1988).
[4] D. Kim, C. H. Skinner, A. Wouters, E. Valeo, D. Voorhees, and S. Suckewer, J. Opt. Soc. Am. B **6**, 115 (1989).
[5] J. C. Moreno, H. R. Griem, S. Goldsmith, and J. Knauer, Phys. Rev. A **39**, 6033 (1989).
[6] T. Hara, K. Ando N. Kusakabe, H. Yashiro, and Y. Aoyagi, Jpn. J. Appl. Phys. **28**, L1010 (1989).
[7] C. J. Keane, N. M. Ceglio, B. J. MacGowan, D. L. Matthews, D. G. Nilson, and D. A. Whelan, J. Phys. B **22**, 3342 (1989).
[8] Z. Z. Xu, Z. Q. Zhang, P. Z. Fan, S. S. Chen, L. H. Lin, P. X. Lu, X. P. Feng, X. F. Wang, J. Z. Zhou, and A. D. Qian, Appl. Phys. B **50**, 147 (1990).
[9] S. S. Chen, Z. Z. Xu, L. H. Lin, P. Z. Fan, and Z. Q. Zhang, Acta Opt. Sin. **10**, 769 (1990).
[10] Z. Z. Xu, P. Z. Fan, Z. Q. Zhang, S. S. Chen, L. H. Lin, P. X. Lu, L. Sun, X. F. Wang, J. J. Yu, and A. D. Qian, in *X-Ray Lasers 1990,* edited by G. J. Tallents, IOP Conf. Proc. No. 116 (Institute of Physics and Physical Society, Bristol, England, 1991).
[11] Z. Z. Xu, Z. Q. Zhang, P. Z. Fan, S. S. Chen, P. X. Lu, X. F. Wang, B. F. Shen, and L. H. Lin, Chin. J. Lasers **1**, 1 (1992).
[12] P. Z. Fan, Z. Q. Zhang, J. Z. Zhou, R. S. Jin, Z. Z. Xu, and X. Guo, Acta Opt. Sin. **12**, 118 (1992).
[13] P. Z. Fan, Z. Q. Zhang, J. Z. Zhou, R. S. Jin, and Z. Z. Xu, Appl. Opt. **31**, 6720 (1992).
[14] X. Q. Zhang, M. X. Gong, Z. H. Cheng, Z. Y. Lei, B. Z. Yang, K. S. Song, and Z. Song, SPIE J. **1032**, 602 (1988).
[15] Y. Kato, E. Miura, T. Tachi, H. Shiraga, H. Nishimura, H. Daido, M. Yamanaka, T. Jitsuno, M. Tagagi, P. R. Herman, H. Takabe, S. Nakai, C. Yamanaka, M. H. Key, G. J. Tallents, S. J. Rose, and P. T. Rumsby, Appl. Phys. B **50**, 247 (1990).

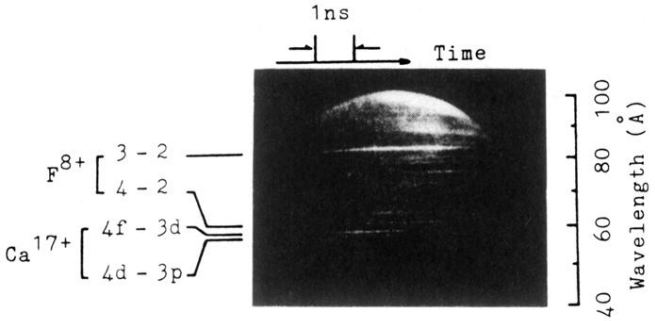

FIG. 4. Axial streaked spectrogram at distance 250 μm from target surface for 10-mm CaF_2 slab target.